Study of Laser Feedback Phase under Self-Mixing leading to Improved Phase Unwrapping for Vibration Sensing

Olivier Bernal, Usman Zabit, Thierry Bosch

Study of Laser Feedback Phase under Self-Mixing leading to Improved Phase Unwrapping for Vibration Sensing

Olivier D. Bernal, Usman Zabit, and Thierry Bosch

***Abstract*—In this paper, the inherent error as well as the robustness of a previously published displacement retrieval technique called the phase unwrapping method (PUM) is analyzed. This analysis, based on a detailed study of laser feedback phase behavior, results in a new algorithm that removes the PUM inherent error while maintaining its robustness. The said algorithm has been successfully tested on simulated and experimental Self-Mixing (SM) interferometric signals. Simulations in weak and moderate feedback regimes demonstrate that the said algorithm can reach a subnanometric precision compared to approximately 25nm for PUM. For experimental SM signals affected by noise, the mesured rms displacement error and the maximum absolute error is approximately 14nm and 37nm respectively for the proposed algorithm and 34nm and 123nm for the PUM, which indicates a three fold displacement precision improvement over the PUM. Finally, it is explained that the precision can be further improved by a reduction of the noise level of experimental SM signals.**

***Index Terms*—Self-Mixing interferometry, laser diode, phase unwrapping method, displacement measurements, moderate regime, weak regime.**

I. Introduction

PHASE retrieval by using the so-called phase unwrapping techniques remains a standard practice in laser sensing. However, in case of Self-Mixing (SM) interferometry [1]–[3], it so appears that a thorough understanding of laser feedback phase under SM condition has not yet been utilized in order to better unwrap the laser phase. So, the present work has been inspired by the idea that a better understanding of the behavior of laser feedback phase would ultimately lead to the design of an improved phase unwrapping method ensuring superior precision.

Displacement retrieval using SM interferometry remains an active area of research [4]–[6] due to the compact, self-aligned and cost-effective nature of a SM sensor. A basic SM sensor resolution of half-wavelength ($\lambda_0/2$) can be easily obtained for a moderate optical feedback level [7]. This basic resolution can be improved either by locking the laser phase to half-fringe through laser diode current modulation compensation loop [8] or by employing phase unwrapping techniques. For example, an unwrapping method is reported in [9] that is based on optical output power (OOP) linearization. Another approach utilizes a direct phase unwrapping of SM signal around signal discontinuities [10]. Yet another unwrapping technique has been presented in [11] that uses a preliminary measurement of two fundamental SM parameters, namely 1) the coupling factor C and 2) the linewidth enhancement factor α. Likewise, [12] proposed a phase unwrapping method (PUM) that allows a joint estimation of C and α, resulting in a measured precision of approximately $\lambda_0/16$.

The aim of this paper is to further improve the retrieval precision of PUM for vibration sensing by deciphering the feedback phase behavior so that subnanometric performance can be achieved. In order to improve PUM, an analysis of the inherent error and robustness of PUM has been carried out in a detailed manner. After a clear identification of the drawbacks and advantages of PUM, an improved phase unwrapping method (IPUM) has been deduced from this thorough PUM theoretical analysis. It will be shown that the IPUM theoretically removes PUM's errors while keeping its inherent robustness. Characteristic SM points (used for the segmentation of SM signals) also recently highlighted in [13], will be clearly identified to lead to better displacement retrieval. However, our approach is based on a detailed study of the behavioural model of SM signals [14] that allows a better understanding of laser feedback phase thereby unveiling the reason behind such a segmentation.

After this analysis of laser feedback phase in the context of its unwrapping for displacement retrieval, simulated and experimental results will be presented. These simulated results will indicate that a subnanometric displacement retrieval precision can be achieved by IPUM in the absence of noise, which is a 25 fold improvement over PUM. In addition, the displacement retrieval results based on experimental SM signals by IPUM and PUM for noise-affected SM signals will both be compared with a reference commercial sensor that indicate a 3 fold improvement of IPUM over PUM. Though IPUM has been designed to process SM signals in the moderate regime, it will be shown that it can be applied to SM signals in weak regime to a certain extent without any changes. Finally, a discussion highlighting the limitation and improvement of the currently implemented version of IPUM for noise affected SM signals will conclude the paper. Let us start with a theoretical backdrop of SM phenomenon.

O. D. Bernal and T. Bosch are with the CNRS, LAAS, F-31400 Toulouse, France and also with the Univ de Toulouse, INP, LAAS, F-31400 Toulouse, France. E-mail: bernal@enseeiht.fr

U. Zabit is with Riphah International University, Islamabad, Pakistan.

Finally, this work might not have been possible had it not been for the funding of the CALDIRO ANR Emergence.

DOI:http://dx.doi.org/10.1109/JSEN.2013.2276106

II. Theory of Self-Mixing

The theory of SM interferometry has been described by various authors [15], [16] and is briefly summarized below. Let $D(t)$ represent the instantaneous distance between the LD driven by a constant injection current and a remote surface that back-scatters a small amount of optical power back into the LD cavity. To highlight the vibration displacement $d(t)$, $D(t)$ can be expressed as follows:

$$D(t) = D_0 + d(t) \tag{1}$$

where D_0 is the distance at rest.

When the optical feedback phenomenon occurs, the laser wavelength is no longer the constant λ_0 but is slightly modified and becomes a function of time $\lambda_F(t)$ varying with $D(t)$. The wavelength fluctuations can be found by solving the phase equation [2]:

$$\begin{aligned} x_0(t) &= x_F(t) + C\sin[x_F(t) + \arctan(\alpha)] \\ &= G[x_F(t), C, \alpha] \end{aligned} \tag{2}$$

where x_F and x_0 represent two phase signals (subject to feedback and under free running conditions, respectively). written as a function of the wavelengths $\lambda_F(t)$ and λ_0, respectively:

$$\begin{aligned} x_F(t) &= 2\pi \frac{D(t)}{\frac{\lambda_F(t)}{2}} = 2\pi \nu_F(t)\tau(t) \\ x_0(t) &= 2\pi \frac{D(t)}{\frac{\lambda_0}{2}} = 2\pi \nu_0(t)\tau(t) \end{aligned} \tag{3}$$

where $\tau(t) = 2D(t)/c$ is the round-trip time and c is the speed of light. $\nu_F(t)$ and ν_0 represent the optical frequencies with and without optical feedback, respectively. C depends notably on the target surface reflectivity and the distance to the remote target. For most sensing applications at present, typical values of C range from 0.1 to 4.6 corresponding to weak and moderate feedback [14]. In this paper, we shall focus on moderate feedback regime (C$>$ 1) as the displacement direction and a rough estimation of the displacement can be easily obtained (it will be later shown that the same technique can be extended for the processing of weak feedback regime signals under certain conditions).

The value of $x_F(t)$ can be extracted from the optical output power (OOP) of the laser diode $P(t)$ using:

$$P(t) = P_0\{1 + m\cos[x_F(t)]\} \tag{4}$$

where P_0 is the power emitted by the free running state laser diode and m a modulation index. Note that the OOP can be recovered by using either the built-in photodiode of the LD package or the LD junction voltage [17]. By using x_F, $x_0(t)$ can first be retrieved using the nonlinear function G (eq.2), which leads to $d(t)$ as demonstrated in [12].

III. PUM Analysis

A. Principle

As previously mentioned, x_F can be extracted from the OOP and more precisely from the normalized OOP (nOOP) $P_N(t)$ given as:

$$\begin{aligned} P(t) &= P_0 + mP_0P_N(t) \\ P_N(t) &= \cos(x_F(t)) \end{aligned} \tag{5}$$

The PUM consists of two principal steps ([12]): (1) a rough estimation $\widehat{x_F}(t)$ of the phase $x_F(t)$, (2) phase correction through the estimation of the C and α parameters in order to recover $x_0(t)$.

It is then possible to apply the arccos function on the nOOP to get $\widehat{x_F}(t)$ mod π. Finally, the unwrapping of the phase estimation $\widehat{x_F}(t)$ is obtained by adding or substracting 2π at the instant of phase discontinuity, depending on the sign of the discontinuity. In [12], it is explained that 2π is chosen as an approximation of $\Delta\Phi$. Then, the second signal processing step consists in estimating the parameters C and α. Finally, an estimation of the retrieved phase $\widehat{x_0}(t)$ based on eq.2 is performed to obtain the displacement d(t).

The PUM employs the arccosine function to process the OOP after normalization. However, this function is only a bijection from [-1;1] toward [0;π]. This implies at least two main consequences on the PUM:

1) Displacement Direction. When the target moves away from the laser, the phase x_0 increases as the distance D(t) becomes longer (eq. 3). From the discontinuity analysis and eq. 2, it can also be shown that if the laser-target distance increases, x_F also increases (see Fig. 2). However, when nOOP increases (right inclined segment in Fig.1, [3]), the obtained phase estimation value $\widehat{x_F}$ decreases due to the use of the arccosine function (eq.4). Therefore, the displacement using the PUM should be inverted in order to obtain the correct displacement direction.

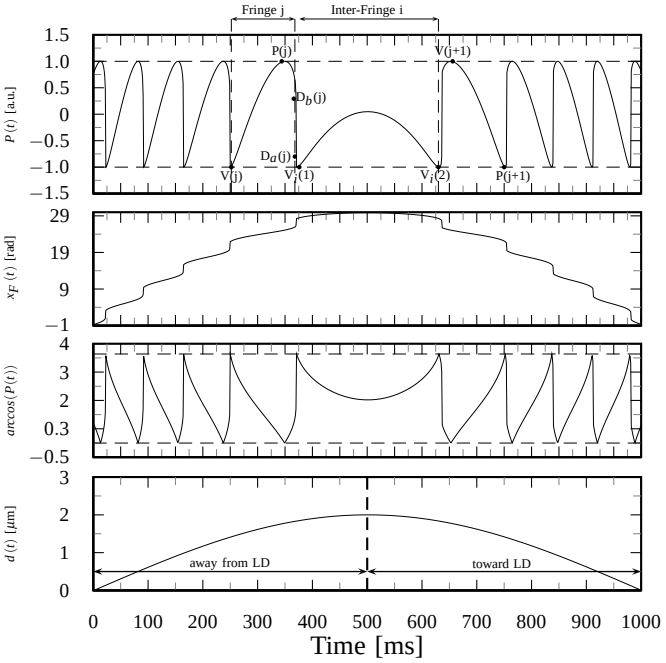

Fig. 1. Graphical representation of a normalized SM signal for C=1.2 and α=3, its corresponding x_F, $arccos(P(t))$ and displacement $d(t)$.

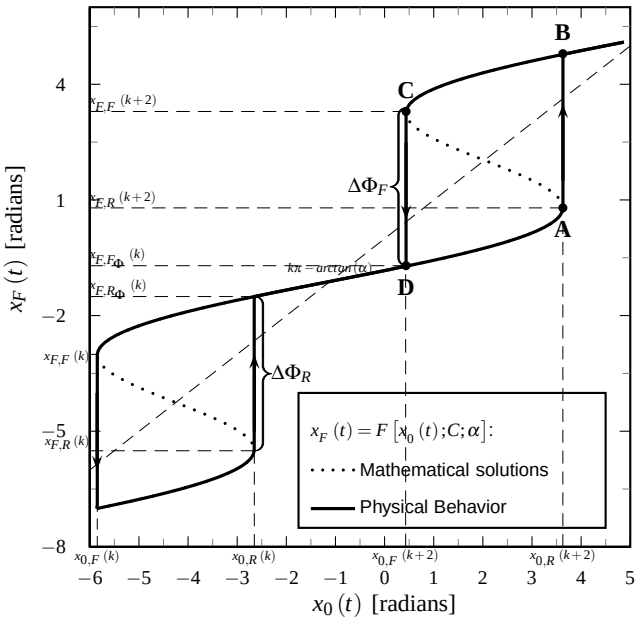

Fig. 2. Transfer function $x_F(t)$=F$[x_0(t);C,\alpha]$ with hysteresis (C=3 and α=2) and k is an even integer.

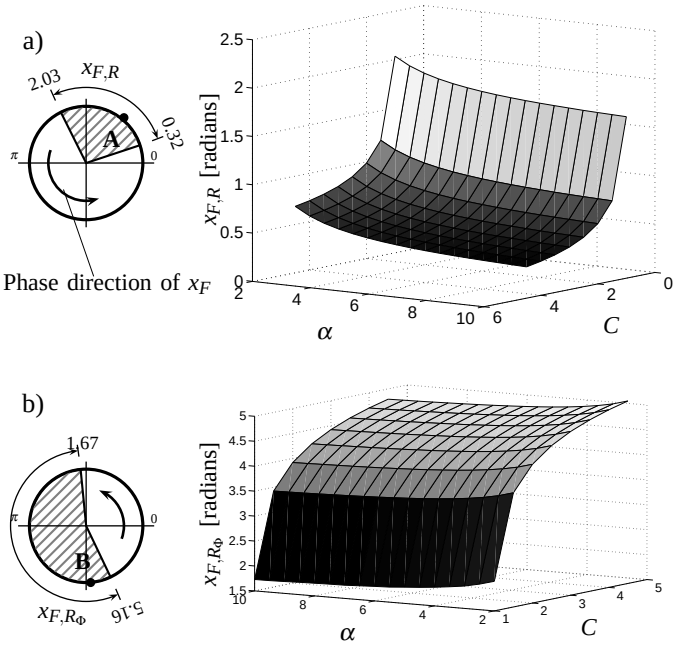

Fig. 3. Graphical representation of the phase value x_F before the rising discontinuity $x_{F,R}$ versus (C;α) (a) and after the rising discontinuity x_{F,R_Φ} versus (C;α) for (C;α)$\in$([1,4.6];]2,10]) .

2) Accurate Phase Discontinuity Retrieval. From the previous algorithm description, one might wonder why once an estimation of C and α is computed, these results are not used to obtain a $\Delta\Phi$ estimation better than 2π and thus a better estimation of $\widehat{x_0}(t)$. So, in order to answer the above question, we need to understand first how $\Delta\Phi$ information is contained in the nOOP signal indicative of laser feedback phase.

B. Feedback Phase Behavior under Self-Mixing

In order to have a better understanding of the phase discontinuity phenomenon, Fig.2 represents the phase of the interference signal x_F as a function of the phase of the ideal signal x_0 (which is also a function of the displacement). Such discontinuities arise from the fact that the function G (see eq. 2) is not invertible when $C>1$ [14]. For such values of C, the laser diode enters into a multiple mode lasing behavior [16]. This results in phase discontinuities and hysteresis phenomena.

Phase discontinuities occur whenever the function $x_F(t) = F[x_0(t),C,\alpha]$ has infinite slopes [14]:

$$x_{F,R} = k\pi - arctan(\alpha) + \beta \quad (6)$$

$$x_{F,F} = (k+2)\pi - arctan(\alpha) - \beta \quad (7)$$

where k is an even integer and β=arccos$\frac{-1}{C}$. These discontinuities can be either rising (subscript R) $\Delta\Phi_R$ or falling (subscript F) $\Delta\Phi_F$ depending on the evolution of $x_F(t)$ (see Fig. 2). It is interesting to note that G presents an inherent symmetry that implies that $\Delta\Phi_R$=$\Delta\Phi_F$=$\Delta\Phi$ (see Appendix A).

Let's have a look at the discontinuity at $x_{F,R}$ (Fig.3 (a)). After the discontinuity, the phase value x_{F,R_Φ} can be estimated numerically (Fig.3 (b)).

From Fig.3 (b), it can be shown that x_{F,R_Φ} is always smaller than 2π if $\alpha > 2$. Therefore, since the arccosine function is only a bijection from [-1;1] to $[0;\pi]$, we have:

$$arccos\left(P_n^{F,R_\Phi}\right) = x_{F,R} + \Delta\Phi \quad \text{if } x_{F,R_\Phi} < \pi \quad (8)$$

$$= 2\pi - (x_{F,R} + \Delta\Phi) \quad \text{otherwise} \quad (9)$$

where P_n^{F,R_Φ} is the nOOP when x_F=x_{F,R_Φ}.

Therefore, two cases have to be considered: (1) $x_{F,R_\Phi} < \pi$ and (2) $\pi < x_{F,R_\Phi} < 2\pi$. In the first case, the estimated phase discontinuity $\Delta\Phi_e$ from the nOOP can be expressed as follows:

$$\Delta\Phi_{e,1} = arccos\left(P_n^{F,R_\Phi}\right) - arccos\left(P_n^{F,R}\right) \quad (10)$$

$$= x_{F,R} + \Delta\Phi - x_{F,R} = \Delta\Phi$$

While, in the second case, we have:

$$\Delta\Phi_{e,2} = 2\pi - (2x_{F,R} + \Delta\Phi) \neq \Delta\Phi \quad (11)$$

Hence, it is obvious that in the first case, $\Delta\Phi$ can be retrieved without any ambiguity while in the second case, it requires the value of $x_{F,R}$.

Let us now have a look at the discontinuity at $x_{F,F}$. In a similar manner to the previous analysis, $\Delta\Phi_e$ can be directly calculated from the nOOP signal. However, here even more cases should be considered since not only $x_{F,F_\Phi} \notin [0;\pi]$, but also $x_{F,F} \notin [0;\pi]$ (see Fig.4).

So, we see that the exact $\Delta\Phi$ value cannot be recovered without any ambiguity for both cases ($\Delta\Phi_R$ and $\Delta\Phi_F$).

Therefore, applying the arccosine function to the nOOP signal is not sufficient in order to correctly recover the phase shift $\Delta\Phi$.

Nevertheless, from the previous analysis, some other relevant information can be extracted regarding the functioning of PUM. It can now be explained why it is relevant to use 2π as $\Delta\Phi$ in PUM.

For the sake of simplicity, we consider here only the case where the target is moving away from the laser, which implies

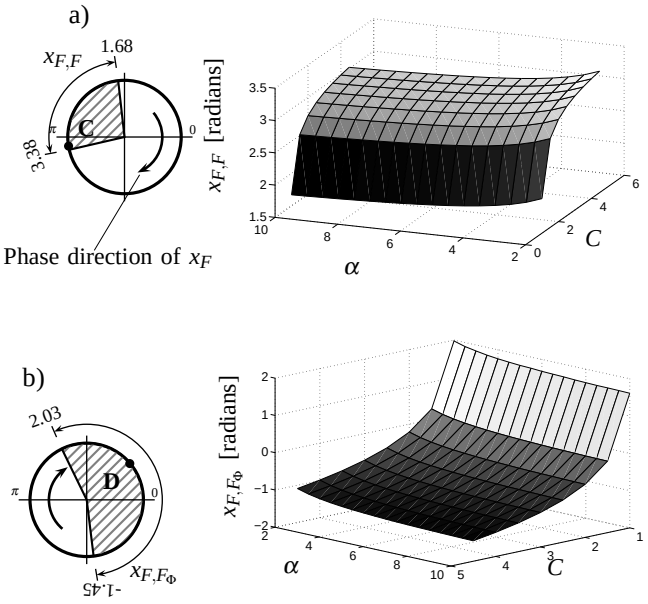

Fig. 4. Graphical representation of the phase value x_F before the falling discontinuity $x_{F,F}$ versus (C;α) (a) and after the falling discontinuity x_{F,F_Φ} versus (C;α) for (C;α)∈(]1,4.6];]2,10]) .

that the phase x_F is increasing. As previously mentioned, when the target is moving away, the phase x_F is increasing so that the nOOP reaches the maximum value (+1) at some time, designated as the peak P (Fig.5). Note again that due to the use of the arccosine function, the PUM interprets it in the opposite way: the phase is decreasing. Therefore, for better understanding, we will use the opposite of the PUM (noted as -PUM) instead of the actual PUM (see Fig. 5) to highligh the other PUM error source. After reaching P, the x_F is still increasing (the target is still moving away) up to $x_{F,R}[2\pi]$. However, after P, the nOOP starts to decrease which implies that by directly using the arccosine function, the phase x_F is wrongly interpreted as decreasing by -PUM. It is mainly this misinterpretation of the PUM that leads to the main displacement error. After the phase discontinuity, x_F reaches x_{F,R_Φ}, which leads to two possible cases: (1) $x_{F,R_\Phi}[2\pi] < \pi$ and (2) $\pi < x_{F,R_\Phi}[2\pi] < 2\pi$.

1) $x_{F,R_\Phi}[2\pi] < \pi$.
   In this case, the -PUM interprets the decreasing nOOP as a decrease of the x_F phase down to -π (Valley point V in Fig.5). Therefore, it can be seen that by adding 2π at the discontinuity, the -PUM arrives at the correct value of x_F after having reached the valley point V (Fig.5). Therefore, the -PUM is able to recover the correct x_F phase evolution except for the region in between P and V. Note that the phase evolution in between P and V can be correctly recovered if $k\pi$ is used as an axis of symmetry (Fig.5).
2) $\pi < x_{F,R_\Phi}[2\pi] < 2\pi$.
   In this case, the -PUM interprets the decreasing nOOP as a decrease of the x_F phase down to -$2\pi + (x_{F_R} + \Delta\Phi)$ according to eq.(9). So, it can be seen that by adding 2π, the correct value $x_{F,R_\Phi} = x_{F_R} + \Delta\Phi$ can be obtained (Fig.6).

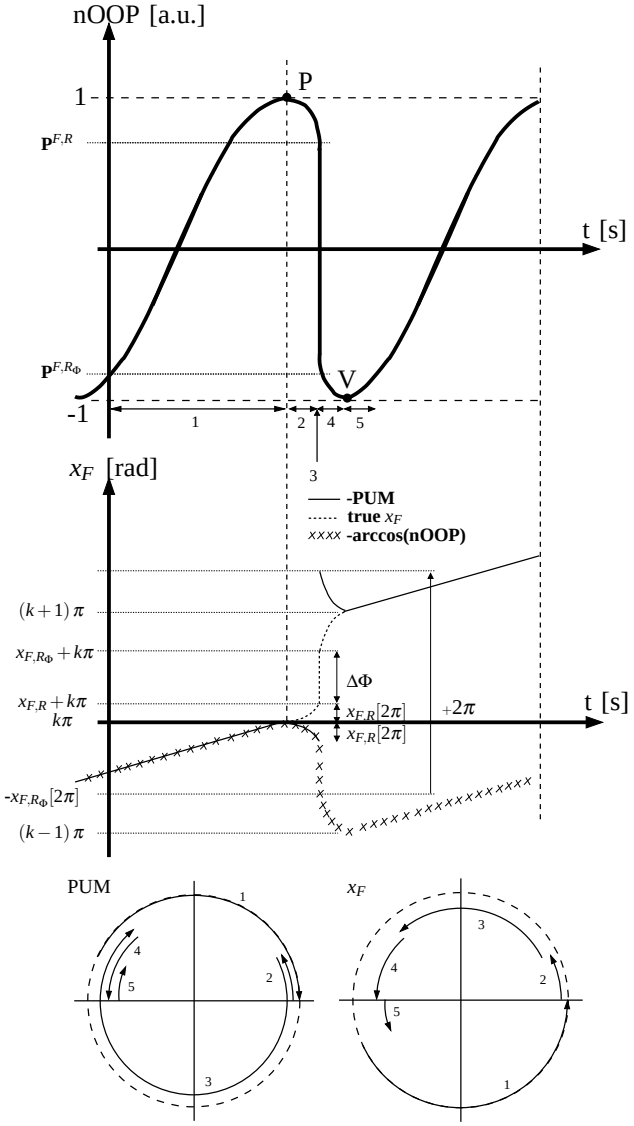

Fig. 5. Graphical representation of the phase value x_F at the discontinuity $x_{F,R}$ for $x_{F,R_\Phi} < \pi$. The graphical circles represent the manner of unwrapping the phase used by the PUM as compared to x_F for $x_{F,R_\Phi} < \pi[k\pi]$.

Therefore, it explains why the use of 2π as $\Delta\Phi$ in the PUM resulted in avoiding any phase drifts that would have occured in the case of use of any other inaccurate $\Delta\Phi$ estimation.

Fig. 5 and Fig. 6 compare the correct evolution of the phase to the PUM based phase assessment. In particular, it shows that the PUM phase sign is opposite to the correct phase and that it changes direction midway instead of unwrapping in the same direction (see the segments 2 and 4 in Fig.5 and the segment 2 in Fig.6).

Note also that inspite of the midway direction changes and the 2π addition inherent in the PUM, the starting and ending points always maintain a phase difference of 2π as is observed for the true x_F. This indicates the absence of accumulation of any phase drift as the PUM moves from one fringe to another, as already detailed. In addition, it explains why using an approximation of $\Delta\Phi$ based on estimated C and α values is not the correct approach due to the possibility of phase

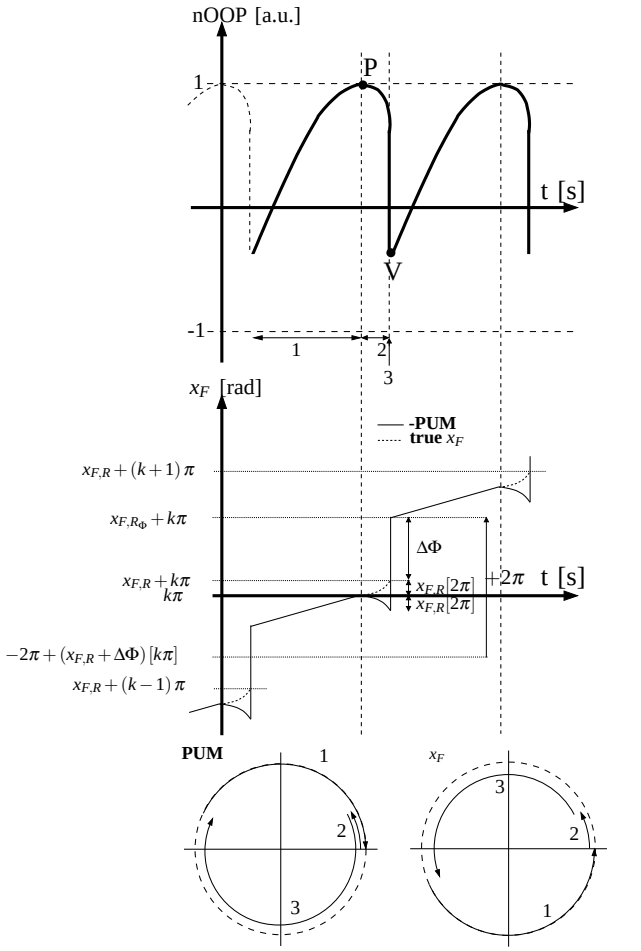

Fig. 6. Graphical representation of the phase value x_F at the discontinuity $x_{F,R}$ for $\pi < x_{F,R_\Phi} < 2\pi$. The graphical circles represent the manner of unwrapping the phase used by the PUM as compared to x_F for $\pi[k\pi] < x_{F,R_\Phi} < 2\pi[k\pi]$.

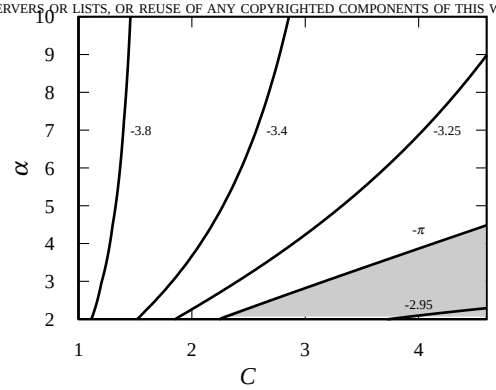

Fig. 7. $x_{F,F}$ versus $(C;\alpha)$ contour plot using Fig.4.

drift. Thus, it can be said that this addition of 2π remains the cornerstone for the PUM.

The previous discussion detailed the case where the target was moving away from the laser. Now, the same analysis can be applied for the case where the target is moving toward the laser and the phase x_F is thus decreasing. Therefore, the previous analysis will be valid if the peak P is now defined as the point at which the nOOP reaches the minimum value and V as the summit point as shown in Fig.1.

In the light of this discussion, let us now present our proposed displacement retrieval algorithm that avoids phase drifts without requiring any $\Delta\Phi$ estimation. More importantly, it is capable of correcting the inherent PUM errors that have been already presented.

IV. Improved Phase Unwrapping Method

The proposed method consists of three main steps which are explained below.

A. Normalization

The very first step of the improved PUM method (IPUM) is similar to the PUM one. It consists in detecting the discontinuities. Once the discontinuities have been detected, it is possible to segment the OOP signal into pieces as mentioned in [13]. Each piece is delimited from the others by its surrounding discontinuities. To the fringe "j" of OOP signal (Fig.1) can be attributed the peak P(j) and the valley V(j) as well as the discontinuity points D_b(j) (before the discontinuity) and D_a(j) (after the discontinuity). Note that an inter-fringe area "i" can be defined in between two successive valleys $V_i(1)$ and $V_i(2)$ delimited by opposite discontinuities.

To normalize the OOP signal, not only the peaks P(j) of the OOP signal should be found but also all the local valleys V(j) should be detected. Knowing these extrema locations allows a better normalization. Note that as previously mentioned, $x_{F,F} \not\subset [0;\pi]$ (see Fig.4 (a)). Therefore, the minimum value -1 is not reach for a certain set $S_{C,\alpha}$ of (C,α) values. The shaded area in Fig.7 shows such a set.

Let us now present the normalisation processing. As previously mentioned, it is known that when the target is moving away from the laser, the nOOP peaks (that are followed by a down-going discontinuity) always reach the value +1 whatever $C \in [1;4.6]$ and $\alpha \in [2;10]$. On the contrary, when the target is moving toward the laser, the nOOP peaks (that are followed by an up-going discontinuity) reach the value -1 except for $S_{C,\alpha}$. The normalization procedure can only be performed if both +1 and -1 values are reached by the SM signal under evaluation. Only this guarantee of +1/-1 allows us to correctly normalize the SM signals by using any/all fringes. Note that this is also applicable for $C < 1$ (weak feedback regime).

Therefore, except for $S_{C,\alpha}$, the normalization should be successful. However, as shown by Fig.3, depending on the value of x_{F,R_Φ} (x_{F,F_Φ}) (and hence on $(C;\alpha)$), the fringe valley V point might not reach -1 (+1). Therefore, correct +1/-1 information guarantee can only be obtained for bidirectional or periodic motion where back and forth motion fringes provide +1 and -1 information respectively. Consequently, the normalisation process cannot be correctly performed for one way linear displacement (the target moves in one direction only) except for such LD regimes for which (C,α) leads to $x_{F,R_\Phi} < \pi$ and $x_{F,F_\Phi} > 0$.

Finally, for the $S_{C,\alpha}$ LD regime, the normalization procedure is much more complex as only +1 information guarantee is available. As a consequence, the normalization of SM signals corresponding to such a set has not been processed for the present study.

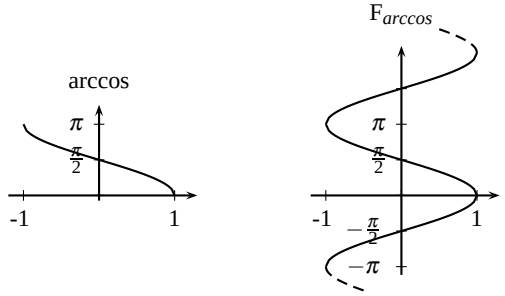

Fig. 8. Graphical representation of the arccosine function and its extended version F_{arccos}.

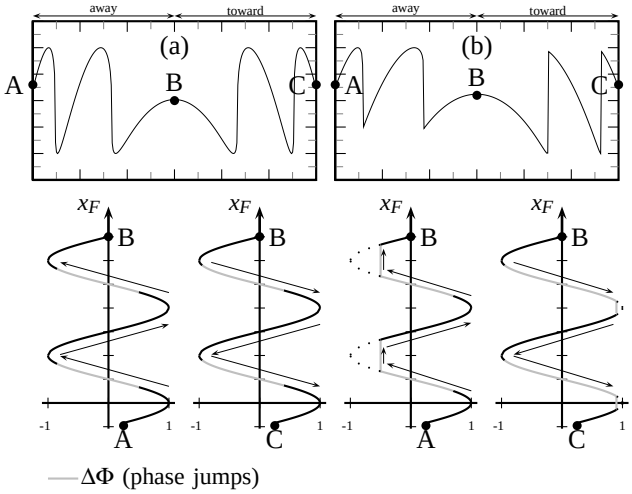

Fig. 9. Illustration of the use of F_{arccos} (Fig. 8) by IPUM for two different SM signals: a) C=1.2 and α=2 (within one fringe +1 and -1 values are reached) and b) C=2 and α=2 (within one fringe only the value +1 or -1 is reached).

B. Unwrapping

After normalizing the OOP, the phase can then be unwrapped. As it was previously shown, the arccosine function (here noted as $f(x)$) cannot be applied directly all over the nOOP (Fig. 8). In addition, it was brought to light that knowing the location of peaks P and valleys V of the SM signals under evaluation is necessary to identify different SM signal segments. Let us summarize below these different segments and how they should be processed.

Firstly, when the nOOP evolves from V to P, in the case of a motion away from (toward) the laser, x_F increases (decreases). Therefore, this segment should be processed using $f(-x)$.

Secondly, when the nOOP evolves from P to V, in the case of a motion away from (toward) the laser, x_F is still increasing (decreasing). Therefore, this segment should be processed using $f(x)$. In addition, by taking into account the fact that $f(x)$ is a bijection toward $[0;\pi]$, in the case of a motion away (toward) from the laser, π should be added to (substracted from) the phase for every change of segment to ensure the function continuity.

Finally, the last segment to be considered is the inter-fringe segment (Fig.1). This one should be simply processed by $f(-x)$ as it is equivalent to the processing of a V to P segment.

Therefore, a function named F_{arccos} can be defined based on the previous description. It is graphically represented in Fig.8.

Fig. 9 shows how the IPUM operates on different SM signals. In Fig. 9 (a), it is obvious that the unwrapping method can be directly based on F_{arccos} as it was shown that $\Delta\Phi$ can be directly extracted from nOOP (see eq.10). Note that such a function could also be applied to weak feedback regime SM signals in order to retrieve the displacement information. This implies that IPUM can be directly used to process weak feedback regime SM signals. It will be shown in the Results section that IPUM can correctly process SM signals with C>0.5. Actually, it is also possible to process SM signals with C<0.5 by modifying the Transition Detector block of IPUM (Fig. 10) in order to cater for the diminished fringe discontinuity of weak SM signals. However, details regarding the processing of weak regime SM signals are not elaborated as it is not the objective of this paper.

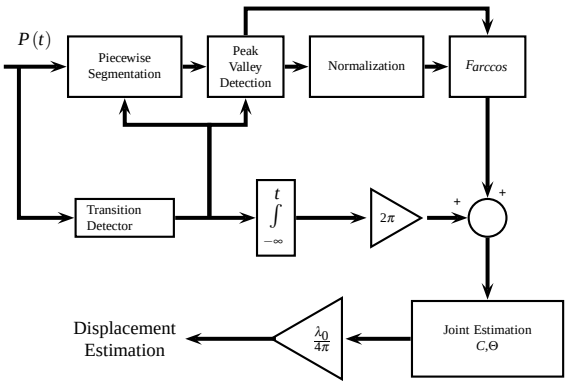

Fig. 10. Principle of signal processing used by IPUM.

In Fig. 9 (b), the same algorithm can also be used. The key point here is to understand that the valley point V corresponds to the end of the phase discontinuity $\Delta\Phi$. In this case, within the discontinuity, x_F crosses $k\pi$ (away) or $(k+1)\pi$ (toward), where k is even. It can thus be compared to a partial fusion of the P-V and V-P segment. Therefore, the F_{arccos} function should be used to unwrap the signal.

Finally, for the $S_{C,\alpha}$, the F_{arccos} function should also be used. The only difference is that $x_{F,F}$ is always greater than $(k+1)\pi$. As previously said, it implies that not only the corresponding peak P is $x_{F,F}$ but also that x_F cannot reach -1 before the discontinuity.

Therefore, based on the discussion detailed above, it can then be stated that F_{arccos} acts as the cornerstone of the IPUM.

C. C and α Joint Estimation

After the correct unwrapping of nOOP, we use the C and α joint estimation processing, as already done for the PUM. Note that the correct unwrapping of nOOP allows us to estimate C and α with a higher precision. This in turn leads to an even better displacement retrieval.

Using such a joint estimation, the C value can be either updated periodically or each time the target changes direction in order to improve the displacement reconstruction accuracy. Note that such a processing does allow measuring target displacement even for those operating conditions where the C value may vary over time.

Finally, the IPUM can be summarized by Fig.10.

TABLE I
C ESTIMATION RESULTS

Actual C	Estimated *C*	Error
0.5	0.503	0.003
1	0.999	0.001
1.5	1.503	0.003
2.5	2.506	0.006
4	4.0014	0.0014

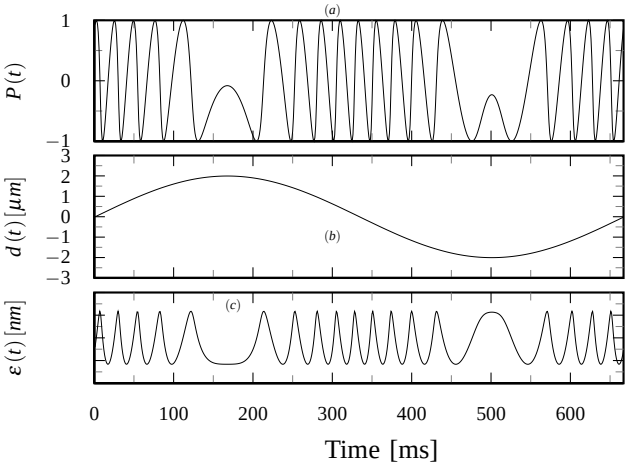

Fig. 11. (a) Simulated optical laser diode output power $P(t)$ for C=0.5, α=2 and λ_0=850nm; (b) Reconstructed target displacement $d(t)$; (c) displacement error for IPUM.

V. RESULTS

A. Simulation

The proposed algorithm has been tested on several simulations. Firstly, simulated sinusoidal displacements with different C values were processed. The results are summarized in Table I.

As previously mentioned, IPUM can process weak regime SM signals to a certain extent (see Table I and Fig. 11).

Then retrieval of arbitrary displacement has also been tested. For this purpose, the considered displacement is a lowpass filtered Gaussian noise [12]. Using the algorithm described in [14], the SM signal corresponding to such a displacement is generated (Fig.12) for C=3 and α=5. The displacement is then retrieved by the proposed IPUM and the error is calculated as the difference between the estimated displacement and the generated one. The estimated root mean square error is approximately 0.25nm for a maximum displacement of 15μm while the error for the same displacement using the standard PUM, is 6.8nm.

It is also interesting to note that the maximum error for the IPUM is approximately 0.8nm while it approximately reaches 25nm for the PUM. This shows that the IPUM can retrieve the target displacement much more accurately than the PUM. Fig.13 shows the difference between the reconstructed x_F by PUM and IPUM.

These simulation results show the improvement brought by IPUM over PUM. It may be added that the residual errors stem from the finite time step used during the simulation that prevents the algorithm from detecting the true P locations.

The presence of noise, however, can directly reduce the displacement retrieval precision (see Fig. 14). It is so because

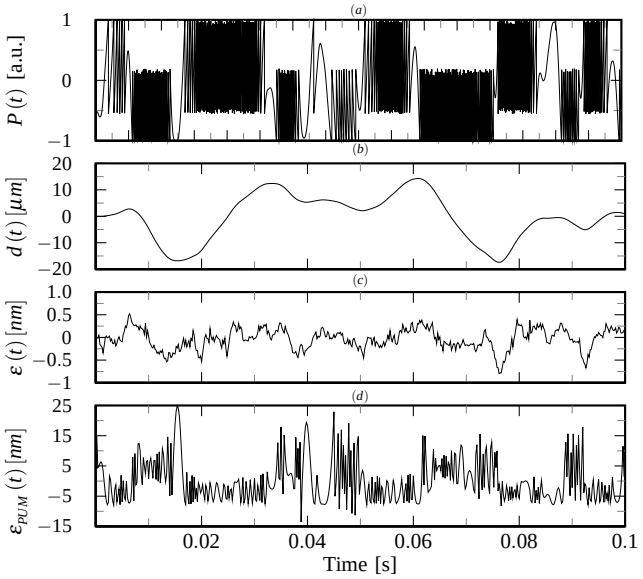

Fig. 12. (a) Simulated optical laser diode output power $P(t)$ for C=3, α=5 and λ_0=785.86nm; (b) Target displacement $d(t)$; Displacement errors for IPUM (c) and PUM (d).

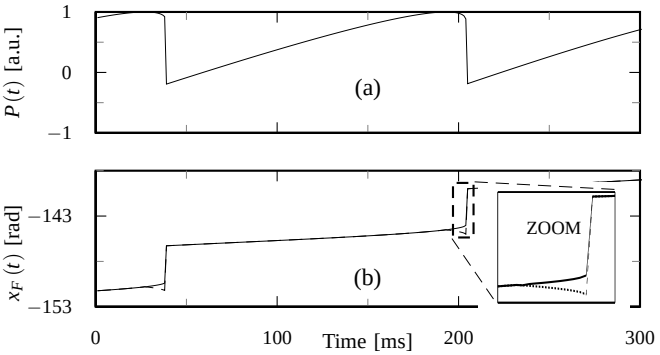

Fig. 13. Simulated OOP fluctuation P(t) (a) for C=3 and α=5 and reconstructed $x_F(t)$ (b) using the PUM ([12]) (dashed curve) and the IPUM (plain) for a a 2μm sinusoidal target displacement $d(t)$ and a laser wavelength of λ_0=850nm.

the presence of noise in SM signals not only results in generating noise on the recovered phase x_F but also causes a jitter in locating true peak P and valley V points. Here, in order to improve the robustness of the IPUM with respect to noise(for the location of P and V), the SM signal has been piecewise approximated by polynomials. Fig. 14 shows the displacement retrieval from a noise affected SM signal. Here, the estimated root mean square error is approximately 9.3nm for a maximum displacement of 4μm. The same behavior has also been observed for experimental SM signals as detailed in the experimental results section.

Finally, the improved precision brought about by IPUM comes at a cost of increased computational time. Simulation results for SM signals with different (C,α) values have shown that on average IPUM requires 50% more computational time than PUM. This extra computational time is mostly needed to determine the P and V locations in a noise-affected SM signal.

B. Experimental Results

The proposed phase unwrapping algorithm has been experimentally tested. The LD used in the SM sensor, driven

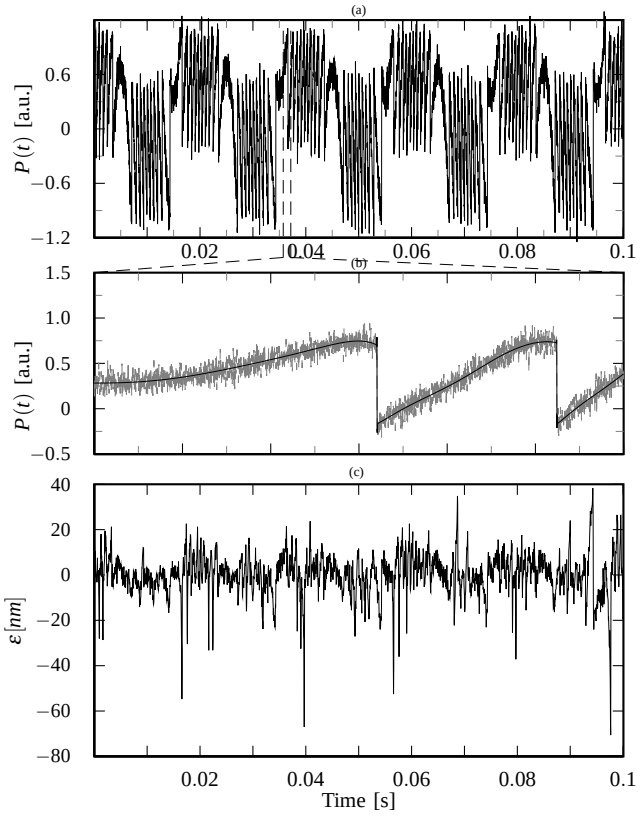

Fig. 14. Simulated noisy OOP fluctuation $P(t)$ for C=3 and α=5. The target displacement $d(t)$ is sinusoidal and the laser wavelength λ_0=785nm. (a): noisy OOP signal; (b): Zoom in OOP signal; (c): Displacement error for the proposed IPUM.

TABLE II
RETRIEVED EXPERIMENTAL DISPLACEMENT ERROR RESULTS

Frequency (Hz)	λ_0 (nm)	PUM (nm)		IPUM (nm)	
		RMS	Peak	RMS	Peak
54	785.86	21	75	8	19
112	787.40	45	165	13	38
80-240	788.83	37	131	21	55
Average	787.36	34	123	14	37

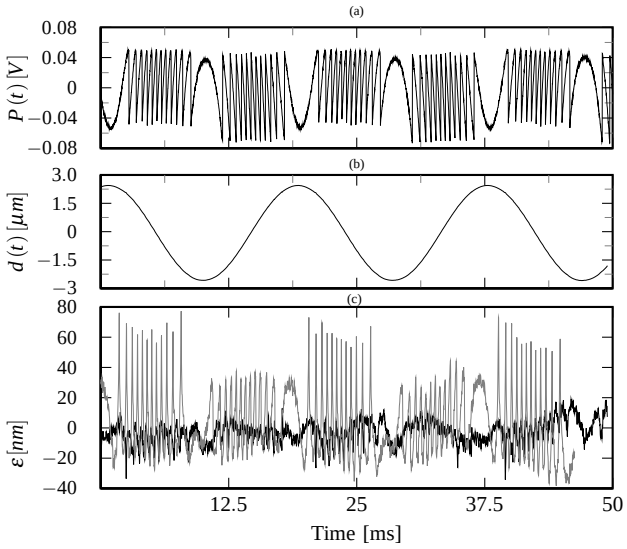

Fig. 15. (a) Experimental OOP $P(t)$ for $d(t)$=2.5$\mu m \times sin(2\pi \times 54 \times t)$ and λ_0=785.86nm; (b): retrieved displacement using IPUM; Displacement errors (c) using IPUM (black) and PUM (gray).

by a constant injection current of 30mA and a maximum output power of 50mW, is a Hitachi HL7851G emitting at λ=785.86nm. The LT110-P collimating lens has a focal length of 6.24mm. A piezoelectric transducer (PZT) from Physik Instrumente (P753.2CD) is used as a target. It is equipped with an internal capacitive feedback sensor (CFS) for direct-motion metrology with a resolution of 2 nm. The CFS output is used as the reference displacement measurement of the real target displacement. In our case, the PZT target has been postioned at 57cm from the SM sensor.

In Fig.15, the PZT is excited at 54Hz with a peak to peak amplitude of 5μm. The corresponding SM signal is indicated in Fig.15 a). The retrieved displacement using IPUM and its corresponding error with respect to CFS are presented in Fig.15 b) and c) (black curve). The corresponding PUM error is also plotted in Fig.15 c) for the sake of comparison (gray curve). The measured rms error of 8nm for IPUM as compared with the measured rms error of 21nm for PUM demonstrates the improvement brought by IPUM. Fig.16 highlights the improved displacement retrieval fidelity of IPUM over PUM for the SM signal already shown in Fig.15.

In Fig.17, the PZT is excited by a signal composed of 80Hz and 240Hz sine waves with a peak to peak amplitude of 5μm. The corresponding SM signal is indicated in Fig.17 a). The retrieved non sinusoidal displacement using IPUM and its corresponding error with respect to CFS are presented in Fig.17 b) and c) (black curve). The corresponding PUM error is also plotted in Fig.17 c) for the sake of comparison (gray curve). The measured rms error of 8nm for IPUM as compared with the measured rms error of 21nm for PUM demonstrates the improvement brought by IPUM.

Table II summarizes the results.

Note that λ_0 was measured (using the WA-1000 wavemeter with a precision of 1pm from Burleigh) for each SM signal acquisition in order to improve the accuracy of the retrieved displacement. Such a measurement is quite important as an error ε_{λ_0} of λ_0 measurement would cause a displacement retrieval error of roughly Nε_{λ_0}, where N is the number of SM fringes.

The reduced precision in displacement measurement based on the experimental SM signal as compared to the results obtained with simulated SM signals is caused by the noise level of experimental SM signals. As previously mentioned, such a noise not only directly affects the estimated phase but more importantly hinders the correct detection of Peaks and Valleys which is essential for a correct normalization of SM signals. This latter effect of noise on IPUM can be observed in the zoomed inset of Fig.16 where a small gap can still be noticed in the IPUM retrieved displacement. In particular, it shows that the maxima or minima (or the peak and valley locations on the SM signal) were not correctly determined due to noise. A reduction of the noise level of experimental SM signals would thus allow even better diplacement retrieval precision.

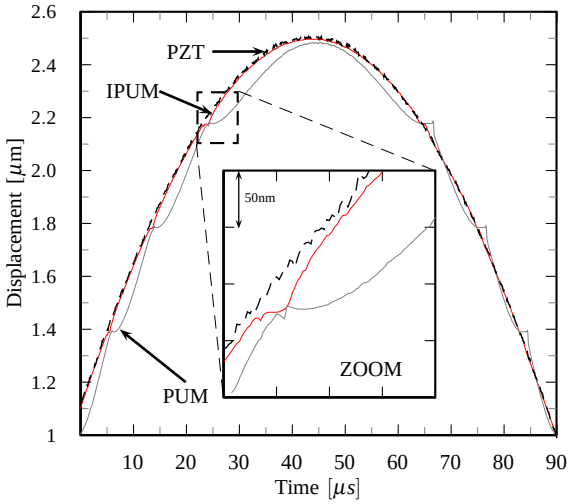

Fig. 16. Comparison of displacement retrieval fidelity for IPUM and PUM with the reference commercial PZT sensor signal.

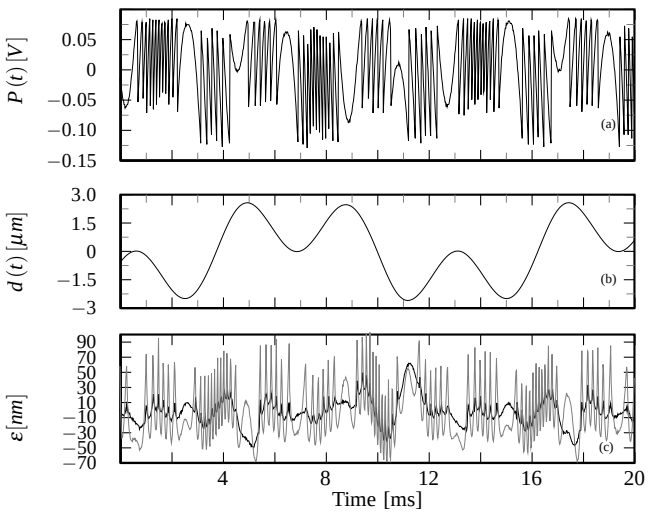

Fig. 17. (a) Experimental OOP $P(t)$; (b): retrieved displacement using IPUM; Displacement errors (c) using IPUM (black) and PUM (gray).

VI. Conclusion

In this paper, after a detailed study of the laser feedback phase behavior under Self-Mixing, the inherent limitations and robustness of the PUM [12] have been brought forth and discussed. In particular, it has been shown that the displacement retrieval using such a method is not only limited by noise but also by the algorithm itself.

Then, it has been shown that the SM signal normalization should be handled with care as it directly affects the displacement retrieval accuracy. Further, it has been demonstrated that such a normalization cannot be accurately performed on the $S_{C,\alpha}$ SM signals.

This has then allowed us to propose IPUM that is based on the detection of Peaks and Valleys of the SM signals and on the use of the F_{arccos} function. Such an approach allows a correct retrieval of the LD feedback phase x_F. As a result of this exact x_F retrieval, the joint estimation of C and α is vastly improved. This in turn further improves the displacement retrieval precision. Such an improvement has been verified for various simulated SM signals in weak and moderate regimes and it has been seen that subnanometer displacement precision can be achieved for simulated SM signals in the absence of noise. Likewise, the IPUM has also provided improved precision as compared to PUM for experimental SM signals. A three fold improvement as compared to the PUM has thus been measured by using a reference commercial sensor. Without any LD temperature control, the measured overall precision is approximately 0.42%. It can be added that a reduction of experimental SM signal noise level would further improve the IPUM displacement measurement precision since in our case, the presence of noise is the primary cause of misinterpretation of laser feedback phase.

Appendix A
Proof of the Inherent Symmetry of G

It is shown in [14] that

$$x_F(t) = x_0(t) = k\pi - atan(\alpha) = x_m^k \ \forall k \in \mathbb{N} \qquad (12)$$

It can then be shown that each x_m^k is a central point of symmetry of x_0.

$$X_r = x_m^k + \delta + C\sin\left(x_m^k + \delta - atan(\alpha)\right) \ \forall k \in \mathbb{N} \ \forall \delta > 0$$

$$X_f = x_m^k - \delta + C\sin\left(x_m^k - \delta - atan(\alpha)\right) \ \forall k \in \mathbb{N} \ \forall \delta > 0$$

$$\forall k \in \mathbb{N} \ \forall \delta > 0 \ \ | X_f - x_m^k | = | X_r - x_m^k |$$

This symmetry implies that $\Delta\Phi_R$=$\Delta\Phi_F$=$\Delta\Phi$.

References

[1] S. Donati, "Developing self-mixing interferometry for instrumentation and measurements," *Laser & Photon. Rev.*, vol. 6, p. 393–417, 2012.

[2] G. Giuliani and S. Donati, *Unlocking Dynamical Diversity - optical feedback effects on semiconductors lasers*, D. M. Cane and K. A. Shore, Eds. John Wiley & Sons, Ltd, 2005.

[3] T. Bosch, C. Bes, L. Scalise, and G. Plantie, *Self-Mixing Sensors*, C. A. Grimes, E. C. Dickey, and M. V. Pishko, Eds. Valencia, CA: American Scientific, 2006.

[4] U. Zabit, O. Bernal, and T. Bosch, "Self-mixing laser sensor for large displacements: Signal recovery in the presence of speckle," *Sensors Journal, IEEE*, vol. 13, no. 2, pp. 824–831, 2013.

[5] R. Atashkhooei, J.-C. Urresty, S. Royo, J.-R. Riba, and L. Romeral, "Runout tracking in electric motors using self-mixing interferometry," *Mechatronics, IEEE/ASME Transactions on*, vol. PP, no. 99, pp. 1–7, 2012.

[6] U. Zabit, O. Bernal, and T. Bosch, "Design and analysis of an embedded accelerometer coupled self-mixing laser displacement sensor," *Sensors Journal, IEEE*, vol. 13, no. 6, pp. 2200–2207, 2013.

[7] S. Ottonelli, F. D. Lucia, M. di Vietro, M. Dabbicco, G. Scamarcio, and F. Mezzapesa, "A compact three degrees-of-freedom motion sensor based on the laser-self-mixing effect," *IEEE Photonics Technology Letters*, vol. 20, no. 16, pp. 1360–1362, Aug. 2008.

[8] G. Giuliani, S. Bozzi-Pietra, and S. Donati, "Self-mixing laser diode vibrometer," *Measurement Science and Technology*, vol. 14, no. 1, p. 24, 2003. [Online]. Available: http://stacks.iop.org/0957-0233/14/i=1/a=304

[9] U. Zabit, F. Bony, T. Bosch, and A. Rakic, "A self-mixing displacement sensor with fringe-loss compensation for harmonic vibrations," *IEEE Photonics Technology Letters*, vol. 22, no. 6, pp. 410–412, 2010.

[10] M. Norgia and A. Pesatori, "Fully analog self-mixing laser vibrometer," *Instrumentation and Measurement Technology Conference (I2MTC), 2011 IEEE*, pp. 1–4, 2011.

[11] S. Donati, G. Giuliani, and S. Merlo, "Laser diode feedback interferometer for measurement of displacements without ambiguity," *IEEE J. Quantum Electron.*, vol. 31, no. 1, pp. 113–119, 1995.

[12] C. Bes, G. Plantier, and T. Bosch, "Displacement measurements using a self-mixing laser diode under moderate feedback," *Instrumentation and Measurement, IEEE Transactions on*, vol. 55, no. 4, pp. 1101 –1105, aug. 2006.

[13] Y. Fan, Y. Yu, J. Xi, and J. F. Chicharo, "Improving the measurement performance for a self-mixing interferometry-based displacement sensing system," *Applied Optics*, vol. 50, no. 26, pp. 5064–5072, 2011.

[14] G. Plantier, C. Bes, and T. Bosch, "Behavioral model of a self-mixing laser diode sensor," *IEEE J. Quantum Electron.*, vol. 41, no. 9, pp. 1157–1167, 2005.

[15] R. Lang and K. Kobayashi, "External optical feedback effects on semiconductor injection laser properties," *IEEE J. Quantum Electron.*, vol. 16, no. 3, pp. 347–355, 1980.

[16] K. Petermann, "External optical feedback phenomena in semiconductor lasers," *IEEE J. Sel. Topics Quantum Electron.*, vol. 1, no. 2, pp. 480–489, 1995.

[17] Y. L. Lim, K. Bertling, P. Rio, J. R. Tucker, and A. D. Rakic, "Displacement and distance measurement using the change in junction voltage across a laser diode due to the self-mixing effect," pp. 60 381O–60 381O–10, 2005. [Online]. Available: +http://dx.doi.org/10.1117/12.638433